View metadata, citation and similar papers at core.ac.uk

brought to you by CORE

provided by Serveur académique lausannois

The Journal of Immunology

This information is current as of July 17, 2020.

Differences in the Transduction of Canonical Wnt Signals Demarcate Effector and Memory CD8 T Cells with Distinct Recall Proliferation Capacity

Caroline Boudousquié, Maxime Danilo, Laurène Pousse, Beena Jeevan-Raj, Georgi S. Angelov, Vijaykumar Chennupati, Dietmar Zehn and Werner Held

J Immunol 2014; 193:2784-2791; Prepublished online 15 August 2014;
doi: 10.4049/jimmunol.1400465
http://www.jimmunol.org/content/193/6/2784

Supplementary Material http://www.jimmunol.org/content/suppl/2014/10/20/jimmunol.1400465.DC1

References This article **cites 21 articles**, 9 of which you can access for free at:
http://www.jimmunol.org/content/193/6/2784.full#ref-list-1

Why *The JI*? Submit online.

- **Rapid Reviews! 30 days*** from submission to initial decision
- **No Triage!** Every submission reviewed by practicing scientists
- **Fast Publication!** 4 weeks from acceptance to publication

**average*

Subscription Information about subscribing to *The Journal of Immunology* is online at:
http://jimmunol.org/subscription

Permissions Submit copyright permission requests at:
http://www.aai.org/About/Publications/JI/copyright.html

Email Alerts Receive free email-alerts when new articles cite this article. Sign up at:
http://jimmunol.org/alerts

The Journal of Immunology is published twice each month by
The American Association of Immunologists, Inc.,
1451 Rockville Pike, Suite 650, Rockville, MD 20852
Copyright © 2014 by The American Association of Immunologists, Inc. All rights reserved.
Print ISSN: 0022-1767 Online ISSN: 1550-6606.

Downloaded from http://www.jimmunol.org/ at Bibliotheque Universitaire de Medecine on July 17, 2020

Differences in the Transduction of Canonical Wnt Signals Demarcate Effector and Memory CD8 T Cells with Distinct Recall Proliferation Capacity

Caroline Boudousquié,* Maxime Danilo,* Laurène Pousse,* Beena Jeevan-Raj,* Georgi S. Angelov,* Vijaykumar Chennupati,[†,‡] Dietmar Zehn,[†,‡] and Werner Held*

Protection against reinfection is mediated by Ag-specific memory CD8 T cells, which display stem cell–like function. Because canonical Wnt (Wingless/Int1) signals critically regulate renewal versus differentiation of adult stem cells, we evaluated Wnt signal transduction in CD8 T cells during an immune response to acute infection with lymphocytic choriomeningitis virus. Whereas naive CD8 T cells efficiently transduced Wnt signals, at the peak of the primary response to infection only a fraction of effector T cells retained signal transduction and the majority displayed strongly reduced Wnt activity. Reduced Wnt signaling was in part due to the downregulation of Tcf-1, one of the nuclear effectors of the pathway, and coincided with progress toward terminal differentiation. However, the correlation between low and high Wnt levels with short-lived and memory precursor effector cells, respectively, was incomplete. Adoptive transfer studies showed that low and high Wnt signaling did not influence cell survival but that Wnt high effectors yielded memory cells with enhanced proliferative potential and stronger protective capacity. Likewise, following adoptive transfer and rechallenge, memory cells with high Wnt levels displayed increased recall expansion, compared with memory cells with low Wnt signaling, which were preferentially effector-like memory cells, including tissue-resident memory cells. Thus, canonical Wnt signaling identifies CD8 T cells with enhanced proliferative potential in part independent of commonly used cell surface markers to discriminate effector and memory T cell subpopulations. Interventions that maintain Wnt signaling may thus improve the formation of functional CD8 T cell memory during vaccination. ***The Journal of Immunology*****, 2014, 193: 2784–2791.**

Protection against intracellular pathogens is chiefly mediated by CD8 T cells. Following an acute encounter with pathogen, very rare naive Ag-specific CD8 T cells expand, differentiate, acquire effector functions, and eventually contain infection. A hallmark of a productive CD8 T cell response is the development of immunological memory, that is, the generation and long-term maintenance of Ag-specific CD8 T cells with efficient re-expansion capacity, which confer improved protection against a secondary encounter with the same pathogen. The complex mechanisms controlling CD8 T cell differentiation are still incompletely understood (1). A better understanding of these processes is essential for the development of novel vaccination strategies to induce protective CD8 T cell memory.

The transcription factors Tcf-1 (*Tcf7*) and Lef-1 play important roles in the generation and/or maintenance of CD8 memory T cells and their function (2–4). In addition to their well-known role as nuclear effectors of the canonical Wnt (Wingless/Int1) signaling pathway, Tcf-1 and Lef-1 repress target genes in the absence of extrinsic Wnt signals. Signaling via the canonical pathway is induced by the presence of extracellular Wnt proteins that induce the intracellular stabilization of β-catenin. As a consequence, β-catenin translocates to the nucleus and associates with the N-terminal domain of DNA-binding Tcf/Lef transcription factors, which mediate the expression of Wnt responsive target genes (5). Consistent with a role for Wnt signal transduction, the formation of functional CD8 T cell memory depended on the presence of the N-terminal catenin binding domain in Tcf-1 and on the expression of β-catenin together with its close homolog γ-catenin (junction plakoglobin) in the hematopoietic compartment (2). However, the absence of β-catenin in CD8 T cells was not limiting for the formation and function of CD8 T cell memory (6, 7). Further, pharmacological inhibition of GSK3β, which activates Wnt signaling, completely suppressed CD8 T cell differentiation in vitro and promoted memory formation (8). However, GSK3β inhibition exerted the same effects in the presence and absence of β-catenin (6), indicating that the effects of pharmacological GSK3β inhibition on CD8 T cell differentiation may not be mediated via the Wnt pathway. It is thus currently not clear whether CD8 T cells transduce canonical Wnt signals under physiological conditions in vivo. Moreover, it is not known whether Wnt signal transduction occurs during a specific phase of an immune response and

*Ludwig Center for Cancer Research, Department of Oncology, University of Lausanne, 1066 Epalinges, Switzerland; [†]Swiss Vaccine Research Institute, Lausanne University Hospital, 1066 Epalinges, Switzerland; and [‡]Division of Immunology and Allergy, Department of Medicine, Lausanne University Hospital, 1066 Epalinges, Switzerland

Received for publication February 20, 2014. Accepted for publication July 11, 2014.

This work was supported in part by a grant from the Swiss National Science Foundation (to W.H.) and a ProDoc program grant from the Swiss National Science Foundation (to W.H. and D.Z.).

The sequences presented in this article have been submitted to Gene Expression Omnibus (www.ncbi.nlm.nih.gov/geo/query/acc.cgi?acc= GSE53358) under accession number GSE53358.

Address correspondence and reprint requests to Prof. Werner Held, Ludwig Center for Cancer Research, Department of Oncology, University of Lausanne, Chemin des Boveresses 155, 1066 Epalinges, Switzerland. E-mail address: Werner.Held@licr.unil.ch

The online version of this article contains supplemental material.

Abbreviations used in this article: IEL, intraepithelial lymphocyte; LCMV, lymphocytic choriomeningitis virus; LPL, lamina propria lymphocyte; MFI, mean fluorescence intensity; MPEC, memory precursor effector cell; pLRP6, phosphorylated LRP6; SLEC, short-lived effector cell; TBP, TATA-binding protein; Tg, transgenic; WT, wild-type.

Copyright © 2014 by The American Association of Immunologists, Inc. 0022-1767/14/$16.00

Downloaded from http://www.jimmunol.org/ at Bibliotheque Universitaire de Medecine on July 17, 2020

whether it is associated with specific properties of CD8 T cells. Finally, even though Tcf-1 plays an essential role in memory formation, it is not known whether Wnt signal transduction in CD8 T cells depends on Tcf-1.

In this article, we have presented a systematic characterization of the dynamics of Wnt signaling in Ag-specific $CD8^+$ T cells during an immune response to an acute viral infection. We find efficient canonical Wnt signaling in all naive cells and progressively in memory $CD8^+$ T cells, whereas short-lived effector cells (SLECs) and effector-like memory cells showed reduced Wnt signaling. Adoptive transfer experiments suggest that maintaining efficient Wnt signal transduction during the primary immune response is associated with an enhanced recall response of memory $CD8^+$ T cells.

Materials and Methods

Mice

The following mouse strains were used: C57BL/6 (B6) mice (Harlan, Horst, the Netherlands); CD45.1 congenic B6 mice (The Jackson Laboratory, Bar Harbor, ME) and bred in house, Tcf-1 knockout (*Tcf7*$^{-/-}$) (B6 backcross > 10) (9) (provided by H. Clevers University of Utrecht, Utrecht, the Netherlands), Tcf7 (p45 isoform) transgenic (Tg) (B6 backcross > 10) (10), P14 TCR Tg (line 327) (B6) (11), OT-1 TCR Tg (12), conductin^{LacZ} (B6) (13) (The Jackson Laboratory); P14 *Tcf7*$^{-/-}$ P14 Cond$^{LacZ/+}$ mice were obtained by breeding. As controls for *Tcf7*$^{-/-}$ mice, we used *Tcf7*$^{+/-}$ or B6 mice (referred to as *Tcf7*$^{+/+}$).

Lymphocytic choriomeningitis virus infection and virus titration

For primary and secondary infections, mice were injected i.v. with 200 and 2000 PFU lymphocytic choriomeningitis virus (LCMV) strain WE, respectively. LCMV titers per gram of spleen weight were determined in centrifuged spleen homogenates, using a plaque-forming assay as described (14).

Flow cytometry

Splenocytes were incubated with anti-CD16/32 (2.4G2) hybridoma supernatant before staining for multicolor flow cytometry with fluorescent mAbs to CD4 (GK1.5), CD44 (IM7), B220 (RA3-6B2), from BD Pharmingen, and CD8α (53-6.7), KLRG1 (2F1), CD62L (MEL-14) and CD127 (A7R34), CD45.1 (A20), CD45.2 (Ali-4A2), CD19 (6D5) from eBioscience. PE-labeled D^b gp33 (KAVYNFATA) tetramers were purchased from TCmetrix (Epalinges, Switzerland).

For intracellular cytokine detection, splenocytes were incubated for 5 h in round-bottom 96-well plates in complete DMEM medium containing Brefeldin A (BioLegend), rIL-2 (50 ng/ml), and gp33 (KAVYNFATM) peptide (400 ng/ml). The cells were harvested, permeabilized, and fixed with BD Cytofix/Cytoperm according to the manufacturer's protocol (BD Pharmingen). After washing, cells were stained with mAbs to IFN-γ (XMG1.2) and IL-2 (JES6-5H4) (eBioscience).

For intranuclear staining, splenocytes were stained for surface markers as described above, then fixed and permeabilized using the Transcription Factor Staining Buffer Set (eBioscience) according to the manufacturer's protocol. Cells were stained with mAbs to TCF-1 (C63D9; Cell Signaling) followed by $F(ab')_2$ anti-rabbit IgG conjugated to PE or FITC (eBioscience) or LEF1 (C12A5) coupled to Alexa 488 (Cell Signaling).

To measure LacZ activity, cells were counted and resuspended at 20×10^6 cells per milliliter in HBSS (Life Technologies) containing 2% FCS, 10 mM HEPES (Life Technologies), and 1% Pen-Strep (Life Technologies). A total of 2×10^6 cells were incubated for 10 min at 37°C and loaded with prewarmed fluorescein di-β-D-galactopyranoside 2 mM (Invitrogen) in H_2O for 1 min. Cells were then transferred to HBSS medium, as indicated above, and left for 90 min on ice before washing and staining for flow cytometry, as described above. Dead cells were excluded using 7-aminoactinomycin D uptake (BioLegend). Samples were run on LSR II or FACSCanto flow cytometers (Becton Dickinson, San Jose, CA) and analyzed using FlowJo software (TreeStar, Ashland, OR).

Cell isolation and adoptive transfers

B cells and CD8 T cells were purified from P14 Tg mice, using EasySep, according to the manufacturer's recommendations (STEMCELL, Vancouver, BC, Canada). Purity of magnetically enriched cells was ∼90%. Purified P14 CD8 T cells (3×10^4 or 10^5) or total splenocytes containing 3×10^4 gp33-specific CD8 T cells were transferred into naive (B6 CD45.1 × B6 CD45.2 Cond$^{LacZ/+}$) F_1 mice by i.v. injection. Female or male mice were used at 6–20 wk of age.

For the isolation of $Cond^+$ and $Cond^-$ cells, purified CD8 T cells were loaded with fluorescein di-β-D-galactopyranoside and stained for CD45.1. Cells were sorted based on detection of LacZ activity in $CD45.1^-$ cells using a FACSAria (Becton Dickinson). The purity of FACS-sorted samples was ∼99%.

For the preparation of intestinal intraepithelial lymphocytes (IELs) and lamina propria lymphocytes (LPLs), the small intestine was extracted and placed in chilled HBSS (+ 5% FBS). The small intestine was flushed with chilled HBSS, and mesentery, fat tissue, and Peyer's patches were removed. The intestine was opened along the mesenteric border, cut into pieces, and incubated in prewarmed HBSS containing 2% FBS, 1 mM DTT (Sigma-Aldrich), and 0.5% EDTA on a shaker (200 rpm) for 40 min at 37°C. The tissue suspension was passed through nylon mesh, and the cells were pelleted at 1200 rpm for 8 min at 4°C. The cell pellet was resuspended in complete RPMI 1640 medium, layered onto a discontinuous 40%/70% Percoll (GE Healthcare) gradient, and centrifuged at 2000 rpm for 20 min at room temperature. Small intestinal IELs were recovered from 40/70% Percoll interface and washed once in complete RPMI 1640. For LPL isolation, the remaining intestinal tissue was washed in complete RPMI 1640 and incubated in prewarmed complete RPMI 1640 medium complemented with collagenase A (1 mg/ml) for 1 h at 37°C. After 10 s vigorous shaking, the cell suspension was filtered through nylon mesh and centrifuged at 1200 rpm for 8 min at 4°C. The cell pellet was subjected to Percoll gradient centrifugation, as described above, and LPLs were recovered from 40/70% interface.

RT–quantitative PCR analysis

Total RNA from cell samples was purified using the TRIzol reagent (Invitrogen). Total RNA was reverse transcribed using random hexamers and SuperScript III First-Strand Kit (Invitrogen). For the PCR, the LightCycler FastStart DNA Master SYBR Green I (Roche Diagnostics) was used according to the instruction manual. The primers used for RT-PCR were the following: Axin2 se, 5′-TGACTCTCCTTCCAGATCCCA-3′; Axin2 anti, 5′-TGCCCACACTAGGCTGACA-3′; TATA-binding protein (TBP) se, 5′-CCTTCACCAATGACTCCTATGAC-3′; TBP anti, 5′-CAAGTTTACAGCCAAGATTCAC-3′. Real-time PCR using SYBR Green was performed on a LightCycler (Roche Diagnostic) according to the manufacturer's instructions. Transcripts were normalized to TBP. Amplification plots were analyzed using the comparative CT method with LightCycler data analysis software, version 3.5 (Roche Diagnostics).

Affymetrix GeneChip

Total RNA was isolated from day 8 sorted P14 $LacZ^+$ and $LacZ^-$ cells using TRIzol (Life Technologies/BRL Life Technologies, Rockville, MD) and RNeasy (QIAGEN) purification following the manufacturers' instructions. cDNA was synthesized and amplified, and samples were hybridized to Affymetrix GeneChip Mouse Gene 1.0 ST array at the Center for Integrative Genomics, University of Lausanne. RNA quality was checked with a Bioanalyzer (Agilent), and cDNA was synthesized. Four sample pairs were hybridized to the microarray for each cell type. Results were analyzed using a linear model, paired analysis. The data were preprocessed with robust multichip average normalization. A Moderated *t* test was used for comparison of the two groups with a *p* value adjustment according to the Benjamini–Hochberg method. Technical replicates were averaged for fold-change study. Probe sets with adjusted *p* value (= false discovery rate) < 0.05 were exported to Microsoft Excel and analyzed further using GeneGO MetaCore analysis software. To test the enrichment of effector/memory genes in $Cond^+$ and $Cond^-$ P14 cells, gene set enrichment analysis was performed as previously described (15). The data discussed in this publication have been deposited in the National Center for Biotechnology Information's Gene Expression Omnibus and are accessible through GEO Series accession number GSE53358 (www.ncbi.nlm.nih.gov/geo/query/acc.cgi?acc= GSE53358).

Western blot

Magnetically enriched B cells and P14 CD8 T cells and FACS-sorted naive or LCMV day 8 P14 CD8 T cells were lysed in the presence of protease and phosphatase inhibitors (Roche), using lysis buffer (Thermo Scientific). Proteins were separated using SDS-PAGE and transferred to nitrocellulose membranes (Bio-Rad). Blots were saturated with 4% dry milk in PBS 1% Tween before incubation with primary Abs: anti-LRP6 (C47E12; Cell

Downloaded from http://www.jimmunol.org/ at Bibliotheque Universitaire de Medecine on July 17, 2020

Signaling), anti-phospho LRP6 (Ser1490; Cell Signaling), anti–β-catenin (clone 14; BD Transduction Laboratory), anti–active-β-catenin (8A7; Millipore), anti–Tcf-1 (C63D9; Cell Signaling), or anti–α-tubulin (B-5-1-2; Sigma-Aldrich). Western blots were revealed with HRP-conjugated anti-mouse and anti-rabbit Abs (Sigma-Aldrich) followed by ECL detection (Pierce).

Statistical analysis

Statistical analyses were performed using GraphPad Prism 5 software using a *t* test. When comparing cell populations within individual mice, a paired *t* test was used (Fig. 2C), and a ratio paired *t* test was used to determine whether cell ratios differed from 1 (Figs. 2F, 3E). Other data were compared using the unpaired Student *t* test. Data sets are considered significantly different when $p < 0.05$ whereby (*), (**), and (***) indicate ($p < 0.05$), ($p < 0.01$), and ($p < 0.001$), respectively, and *ns* is $p > 0.05$.

Results

Wnt signal transduction during CD8 T cell differentiation

To determine Wnt signal transduction in CD8 T cells at the single-cell level, we used mice in which the endogenous open reading frame of one conductin (*Axin2*) allele was replaced with a bacterial β-galactosidase (LacZ) reporter gene (termed Cond^{LacZ}) (13). Because conductin is a direct target gene of Tcf-1 in CD8 T cells (3), we used ex vivo LacZ activity to follow Wnt signal transduction at the single-cell level. Significant LacZ activity was observed in CD8 T cells of naive mice. The signal was equal in naive (CD44^{lo}) and memory (CD44^{hi}) CD8 T cells, but was not detected in B cells (Fig. 1A). Similar results were obtained using naive CD8 T cells expressing known TCR specificities for LCMV gp33/H-2D^{b} (P14) (Fig. 1B) or OVA/H-2K^{b} (OT-1) (not shown), demonstrating that Ag-unexperienced CD8 T cells with defined TCR specificity display constitutive Wnt reporter activity.

We next addressed Wnt signal transduction during the CD8 T cell response to an acute LCMV infection. P14 Cond^{LacZ} CD8 T cells (CD45.2) were adoptively transferred into wild-type (WT) recipients (CD45.1^{+}CD45.2^{+}), and LacZ activity was assessed at various time points following LCMV infection. At day 8 post infection, the majority of P14 cells were LacZ^{-}; however, a subset of ~30% of P14 cells retained LacZ activity (Fig. 1B). Corresponding LacZ activity patterns were observed among polyclonal CD8 T cells specific for the LCMV epitopes gp33 (Fig. 1C), NP396, and NP205 (Supplemental Fig. 1A), indicating that conductin downregulation is also a feature of a polyclonal CD8 T cell response. In addition, LacZ downregulation activity was observed in OT-1 T cells during infection with *Listeria monocytogenes* expressing OVA (not shown), suggesting that the emergence of the two effector populations is independent of the type of acute infection.

Following the peak of the CD8 T cell response and the contraction phase, the fraction of LacZ^{+} P14 cells gradually increased and LacZ activity was eventually detected in most P14 memory cells present in the blood, the spleen, and the lymph node (Figs. 1B, 2E and not shown). Thus, between day 8 and >day 60 post infection, LacZ^{+} P14 cells contracted less prominently. compared with LacZ^{-} P14 cells (Fig. 1D). A progressive increase in the fraction of LacZ^{+} cells was also observed among polyclonal CD8 memory T cells specific for the gp33 LCMV epitope (Fig. 1C).

To ascertain whether LacZ activity reflected expression of the endogenous *Axin2* gene, we sorted WT P14 cells on day 8 and > day 40 following LCMV infection and determined *Axin2* mRNA by quantitative RT-PCR. *Axin2* mRNA expression was below detection in B cells, high in naive P14 T cells, reduced at the peak of the CD8 T cell response, and partially restored in LCMV immune P14 cells (Fig. 1E), which readily corresponded to the activity of the Cond^{LacZ} reporter described above.

To obtain independent evidence that the canonical Wnt signaling pathway was active in CD8 T cells, we also tested an artificial

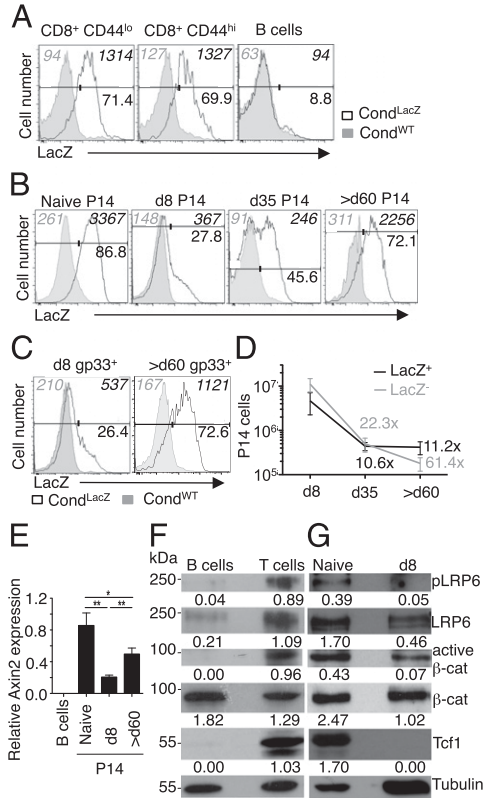

FIGURE 1. Conductin expression during CD8 T cell differentiation. (**A**) Histograms show LacZ activity in naive (CD44^{low}) and memory-like (CD44^{high}) CD8^{+} T cells and in B cells from naive Cond^{LacZ} (open histogram) compared with Cond^{WT} mice (gray fill). Roman numbers indicate the percentage of LacZ^{+} cells, and italic numbers depict the MFI of LacZ staining of the corresponding populations (gray for Cond^{WT} and black for Cond^{LacZ} cells). (**B**) LCMV gp33-specific P14 CD8 T cells (3×10^{4}, CD45.2) were adoptively transferred into CD45.1/2 recipient mice prior to LCMV infection. Histograms show LacZ activity in P14 Cond^{LacZ} (open histogram) compared with P14 Cond^{WT} control cells (gray fill), prior to infection (Naive) and at day 8 (d8), d35, and >d60 following LCMV infection. (**C**) Histograms show LacZ activity in polyclonal gp33 tetramer^{+} CD8 T cells from Cond^{LacZ} (open histogram) compared with Cond^{WT} mice (gray fill) at d8 and >d60 following LCMV infection. (**D**) The graph depicts the abundance of LacZ^{+} (black line) and LacZ^{-} P14 cells (gray line) present in the spleen after LCMV infection. Numbers indicate the fold contraction from d8 to d35 and from d8 to >d60 following LCMV infection. (**E**) Quantitative RT-PCR analysis of *Axin2* gene expression in B cells, in naive P14 cells, and at d8 and >d60 following LCMV infection. (*) and (**) depict significant differences ($p < 0.05$) and ($p < 0.01$), respectively, based on the Student *t* test. Cell lysates from equal numbers of B cells and T cells from naive mice (**F**) and from equal numbers of naive and d8 P14 cells (**G**) were analyzed by Western blot for pLRP6 and nonphosphorylated, active β-catenin. Numbers indicate protein abundance relative to Tubulin.

lentivirus reporter system in which a fluorescent protein is under the control of multimerized TCF/LEF binding sites (16). However, this system was not sensitive enough to detect physiological Wnt levels during CD8 T cell differentiation (not shown). We thus assessed the presence of phosphorylated LRP6 (pLRP6) and of nonphosphorylated (active) β-catenin, two hallmarks of active signal transduction via the canonical Wnt pathway. In agreement with the reporter analysis, Western blots readily identified pLRP6 and active β-catenin in naive total T cells and in P14 cells, but not in B cells (Fig. 1F, 1G). At day 8 of the immune response to LCMV infection, pLRP6, active β-catenin and Tcf-1 were all severely downregulated in P14 cells (Fig. 1G). These data validate

Downloaded from http://www.jimmunol.org/ at Bibliotheque Universitaire de Medecine on July 17, 2020

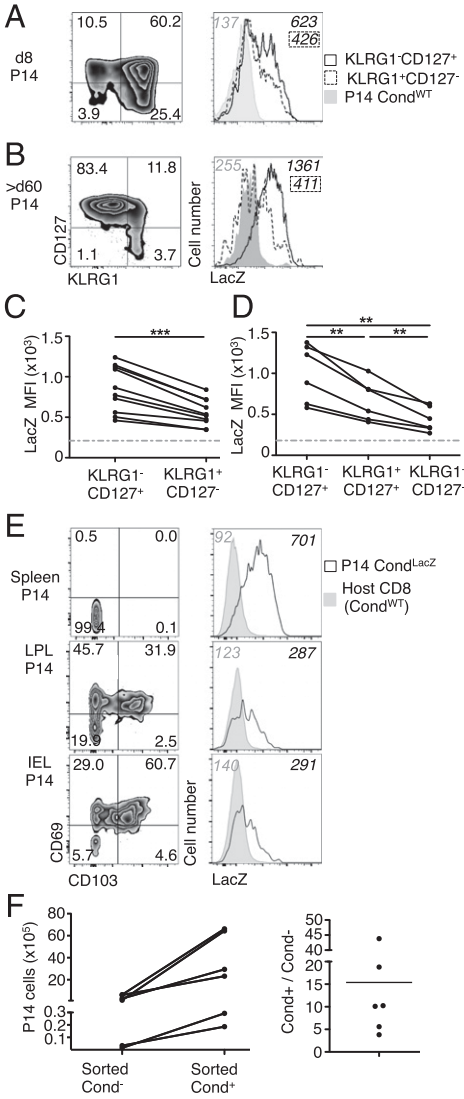

FIGURE 2. Phenotype and function of Cond$^+$ and Cond$^-$ memory CD8 T cells. Purified Cond^{LacZ} or Cond^{WT} P14 cells (10^5, CD45.2) were transferred into WT (CD45.1/2) recipients followed by LCMV infection 1 d later. (**A**) Recipient mice were analyzed at day 8 (d8) post infection. Density plots show the expression of CD127 versus KLRG1 in donor-derived (CD45.2$^+$0.1$^-$) CD8$^+$ cells. Histograms show LacZ activity (Cond expression) in the indicated population of cells. Roman numbers indicate the percentage of cells in the respective gates or quadrants; italic numbers indicate the MFI of LacZ staining. (**C**) The line graph depicts the MFIs of LacZ staining in the indicated population of cells in individual mice (connected with a line). (**) and (***) depict significant differences ($p < 0.01$) and ($p < 0.001$), respectively, based on the paired Student t test. (**B** and **D**) Same analysis as above at >d60 post infection. (**E**) Density plots show the expression of CD103 versus CD69 in donor-derived (CD45.2$^+$0.1$^-$) CD8$^+$ cells present among splenocytes, LPLs, and IELs of the small intestine at >60 d after LCMV infection. Histograms show LacZ activity in P14 cells (Cond^{LacZ}) relative to host CD8 T cells (Cond^{WT}) in all P14 cells present in the spleen compared with gated CD103$^+$CD69$^+$ LPLs and IELs. Data are representative of four independent analyses. (**F**) Cond$^+$ and Cond$^-$ P14 Cond^{LacZ} cells (CD45.1$^-$) were flow sorted from individual primary recipient mice at d35 after LCMV infection, and 5×10^3 cells were transferred into naive secondary recipients (CD45.1/2) followed by LCMV challenge infection. The number of donor-derived P14 cells was determined 5 d later. Data deriving from the same primary donor are connected with a line (*left*) and were used to calculate a fold difference in the expansion of Cond$^+$ versus Cond$^-$ P14 cells (*right*), which is statistically significant ($p < 0.01$) based on ratio paired Student t test.

the reporter analysis shown above and provide an explanation for the reduced LacZ activity at the peak of the immune response. We conclude that naive CD8 T cells constitutively transduce canonical Wnt signals and that Wnt signaling is extinguished in most, but not all, effector cells and is present in the majority of memory cells.

Phenotype and function of conductin$^+$ memory CD8 T cells

We next determined whether Wnt signal transduction correlated with the expression of cell surface markers commonly used to discriminate effector and memory CD8 T cell subsets. At day 8 following LCMV infection, memory precursor effector cells [(MPECs), KLRG1$^-$CD127$^+$] displayed, on average, 2-fold higher Cond expression [based on the quantification of the LacZ mean fluorescence intensity (MFI)], compared with SLECs (KLRG1$^+$ CD127$^-$) (Fig. 2A, 2C). At the memory stage (>day 60), KLRG1$^-$CD127$^+$ CD8 cells displayed significantly higher Cond expression, compared with KLRG1$^+$CD127$^-$ cells (3- to 4-fold following background subtraction), whereas KLRG1$^+$CD127$^+$ cells had intermediate Cond levels (Fig. 2B, 2D). The discrimination of Cond$^+$ and Cond$^-$ CD8 T cells could not be improved further using additional cell surface markers (including CD62L, CD27, Ly6C) and combinations thereof (not shown). Compared with Cond expression in memory cells present in lymphoid tissues, Cond expression was low in CD103$^+$ tissue-resident P14 memory cells present in the lamina propria or among IELs of the small intestine (Fig. 2E). Thus, Wnt signal transduction was preferentially reduced among terminally differentiated SLECs and effector-like memory CD8 T cells.

To test whether the intensity of Wnt signaling discriminated between memory cells with distinct properties, we separated Cond$^+$ and Cond$^-$ memory cells from lymphoid tissues using flow sorting (Supplemental Fig. 1B). Upon restimulation, Cond$^+$ memory cells, compared with Cond$^-$ memory cells, produced more IL-2 (not shown). Next, equal numbers of sorted P14 Cond$^+$ and Cond$^-$ memory cells were transferred into naive recipient mice. The next day, recipients were infected with a high LCMV dose. At day 5 after rechallenge, descendants of the transferred Cond$^+$ and Cond$^-$ P14 memory cells had a comparable CD127$^-$ KLRG1$^+$ population (Supplemental Fig. 1C), indicating that both types of cells can give rise to SLECs during a secondary response. However, Cond$^+$ sorted P14 cells expanded, on average, 15-fold more efficiently than Cond$^-$ P14 cells ($n = 6$) (Fig. 2F). We conclude that efficient Wnt signaling delineates memory CD8 T cells with an increased capacity to re-expand.

Fate and functional properties of conductin$^+$ effector CD8 T cells

During the primary immune response, Cond expression was reduced in the majority of day 8 effector cells (Fig. 1B). Efficient Cond downregulation was observed after day 6 of LCMV infection (Supplemental Fig. 1D) and after day 5 of *L. monocytogenes* infection (not shown). These data indicate that Cond loss is a late event during effector differentiation, independent of the initial clonal burst or the acquisition of effector function. We thus sorted day 8 Cond$^+$ and Cond$^-$ P14 cells (Fig. 3A) and compared their gene expression profiles. On the basis of four independent data sets, 537 of 28,000 genes were differentially expressed (adjusted $p < 0.05$). A total of 456 genes were upregulated and 81 genes were downregulated in Cond$^+$ compared with Cond$^-$ P14 cells. The array analysis showed that genes associated with a central memory differentiation program [such as *Ccr7*, *Sell* (CD62L), and *IL7Rα* (CD127)] were expressed at higher levels in Cond$^+$ P14 cells,

Downloaded from http://www.jimmunol.org/ at Bibliotheque Universitaire de Medecine on July 17, 2020

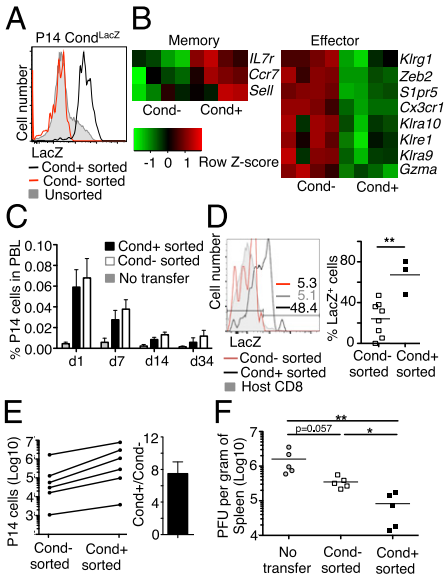

FIGURE 3. Function and fate of Cond$^+$ and Cond$^-$ effector CD8 T cells. Purified P14 Cond^{LacZ} CD8 T cells (10^5, CD45.2$^+$) were transferred into WT recipients (CD45.1/2) followed by LCMV infection 1 d later and analysis 8 d later. (**A**) Histogram overlays show P14 Cond^{LacZ} cells before (gray fill) and after sorting into Cond$^+$ (black line) and Cond$^-$ cells (red line). (**B**) The heat maps show the expression of selected genes associated with CD8 memory (*left*) or effector differentiation (*right*) among day 8 sorted Cond$^+$ and Cond$^-$ P14 effector cells. (**C**) Day 8 sorted Cond$^+$ and Cond$^-$ P14 cells (10^6) were transferred into naive secondary recipients. The bar graph shows the mean percentage (±SD) of transferred cells (CD45.2$^+$CD45.1$^-$CD8$^+$ T cells) among PBLs at the indicated time point following cell transfer. Background was determined using non-transferred mice (No transfer). (**D**) The histogram overlays show LacZ activity in P14 day 8 sorted as Cond$^+$ (black line) and Cond$^-$ (red line) cells as compared with the background activity of host CD8 cells (gray fill) 7 d (d7) after transfer. The dot graph shows the percentage of Cond$^+$ P14 cells derived from day 8 sorted Cond$^+$ and Cond$^-$ cells. Each symbol represents data from an individual mouse. (**E**) LCMV challenge infection of recipient mice 25 d after the adoptive transfer of day 8 sorted Cond$^+$ and Cond$^-$ P14 cells (10^6). At 5 d post infection, the absolute number of donor-derived cells was determined. Data derived from the same primary donor are connected with a line (*left*) and were used to calculate a fold difference in the expansion of Cond$^+$ versus Cond$^-$ P14 cells (*right*), which is statistically significant ($p < 00.1$) based on ratio paired Student *t* test. (**F**) Recipient spleens were analyzed for infectious LCMV particles PFUs. (*) and (**) depict significant differences ($p < 0.05$) and ($p < 0.01$), respectively, based on the paired Student *t* test.

whereas genes associated with effector differentiation [including *Klrg1*, *Zeb2*, *S1pr5* (17); *Cx3cr1* (17); *Klra10*, *Klre1*, *Klra9*, and *GzmA*] were enriched in Cond$^-$ P14 cells (Fig. 3B).

We used gene set enrichment analysis for an unbiased identification of signatures associated with Cond$^+$ and Cond$^-$ cells. This analysis revealed that Cond$^-$ cells express genes that are upregulated in IL-7R^{low} effector cells (compared with IL-7R^{high} cells) (18)($p < 0.001$, Supplemental Fig. 2A) and that genes downregulated in memory cells (versus KLRG^{high} effector cells) are significantly enriched among Cond$^+$ cells (false discovery rate < 25%) (19)(Supplemental Fig. 2B). Pathway analysis using GeneGo revealed a highly significant upregulation of genes involved in cell cycle progression (Supplemental Fig. 2C), including cyclins, cyclin-dependent kinases, and related genes, in Cond$^+$ effector cells. However, the overexpression of cell cycle genes was not associated with increased proliferation (7.3 ± 2.4% of Cond$^+$ versus 5.9 ± 2.5% of Cond$^-$ cells ($p = 0.38$) were in the S, G2, and M phases of the cell cycle). Enhanced expression of cell cycle regulatory genes may allow Cond$^+$ cells to more rapidly re-enter the cell cycle upon restimulation, which is a hallmark of central CD8 T cell memory (20, 21). We conclude that Cond$^+$ effector cells display a gene expression program, which is consistent with central memory differentiation.

To address the fate of the two effector populations, flow sorted Cond$^+$ and Cond$^-$ P14 CD8 T cells from day 8 LCMV-infected mice were adoptively transferred into naive or infection-matched recipient mice. Cond$^+$ and Cond$^-$ P14 cells persisted comparably in naive (Fig. 3C) or in infection-matched recipient mice (Supplemental Fig. 2D), suggesting that Wnt signaling does not confer a survival advantage. After transfer, the majority of the Cond$^+$ and Cond$^-$ P14 cells were CD127$^+$ KLRG1$^-$ (Supplemental Fig. 2E), which is in agreement with the fact that KLRG1$^+$ cells are predominantly short lived (18, 19). Transferred Cond- P14 effector cells remained predominantly Cond$^-$, whereas Cond$^+$ P14 effectors remained mostly Cond$^+$ in either infection-matched (Supplemental Fig. 2F) or naive recipients (Fig. 3D). Thus, following transfer, the Wnt phenotype of effector CD8 T cells was relatively stable. Clearly, however, Cond$^+$ CD8 cells can give rise to Cond$^-$ cells during a primary (Fig. 1B) or a secondary (Supplemental Fig. 1C) immune response.

We next determined the re-expansion and protective capacity of descendants of transferred Cond$^+$ and Cond$^-$ day 8 effector cells. At 25 d after transfer, naive recipient mice were challenged with a high-dose LCMV infection, and the recall response was evaluated 5 d later. Descendants of the transferred Cond$^+$ and Cond$^-$ P14 cells were predominantly Cond^{low} (not shown) and KLRG1^{high} (Supplemental Fig. 2G), indicating that both populations produced differentiated cells during a secondary response. However, progeny of Cond$^+$ P14 effector cells showed, on average, a 7-fold higher re-expansion than progeny of Cond$^-$ cells ($n = 6$) (Fig. 3E). Finally, progeny of Cond$^+$ P14 effector cells conferred a significantly better control of virus infection than did Cond$^-$ P14 cells (Fig. 3F). We conclude that the loss of Wnt signal transduction during the primary immune response does not preclude memory formation and that such cells display effector memory function. In contrast, the maintenance of Wnt signal transduction during the primary immune response is associated with the differentiation into memory cells with enhanced proliferative potential and improved protective capacity.

Tcf-1 ensures efficient Wnt signal transduction in memory CD8 T cells

Canonical Wnt signals are transduced using nuclear effectors of the TCF/LEF family of transcription factors. Because Tcf-1 plays an essential role in the formation of CD8 T cell memory (2, 3) we assessed whether and at what stage Tcf-1 contributed to Wnt signal transduction during CD8$^+$ T cell differentiation. Tcf-1–deficient P14 cells mounted a normal primary immune response to LCMV infection (Fig. 4A, not shown) (2), and they yielded the same Cond-defined effector subsets seen using WT P14 cells (Fig. 4A). Thus, the absence of Tcf-1 was not limiting for Wnt signal transduction during the primary immune response. Low levels of Lef-1 were expressed by a subpopulation of Tcf-1 knockout effector cells (Supplemental Fig. 3A), suggesting that Wnt signal transduction in the absence of Tcf-1 may be mediated by Lef-1.

In contrast to the effector stage, Wnt signaling was significantly reduced when memory P14 cells lacked Tcf-1 (Fig. 4B, 4C). Among effector-like memory cells (CD127$^-$KLRG1$^+$ and CD127$^+$KLRG1$^+$), the relatively low Cond levels were unaltered (Fig. 4B, 4C), and these cells were equally abundant in the presence and absence of Tcf-1 in P14 cells (Fig. 4D). In contrast,

Downloaded from http://www.jimmunol.org/ at Bibliotheque Universitaire de Medecine on July 17, 2020

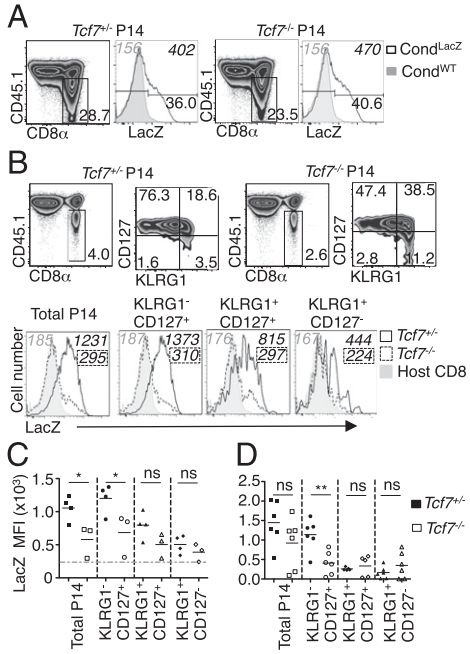

FIGURE 4. Tcf-1 defciency reduces Wnt signaling in memory CD8 T cells. Purified CD8 T cells from *Tcf7*$^{-/-}$ and from *Tcf7*$^{+/-}$ P14 Cond^{LacZ} mice (3×10^4, CD45.2$^+$) were transferred into WT recipients (CD45.1/2) followed by LCMV infection 1 d later. (**A**) Dot plots and histogram overlays show Cond expression (LacZ activity) in gated *Tcf7*$^{-/-}$ and *Tcf7*$^{+/-}$ P14 Cond^{LacZ} cells (CD45.1$^-$CD8$^+$) (open histogram) compared with background derived from host CD8 cells (Cond^{WT}, gray fill). Roman numbers indicate the percentage of cells in the respective gates or quadrants, and italic numbers depict the MFI of LacZ staining. (**B**) Density plots show the expression of CD127 versus KLRG1 among gated *Tcf7*$^{-/-}$ and *Tcf7*$^{+/-}$ P14 Cond^{LacZ} (CD45.1$^-$CD8$^+$) cells at >day 60 after LCMV infection. Histogram overlays show Cond expression in the indicated subset of *Tcf7*$^{-/-}$ (dashed line) and *Tcf7*$^{+/-}$ P14 Cond^{LacZ} cells (black line) compared with background activity in host CD8 cells (Cond^{WT}) (gray fill). Italic numbers depict the corresponding MFI of LacZ staining. (**C**) Cond levels (as indicated by the MFI of LacZ staining) in the indicated memory subpopulations of *Tcf7*$^{-/-}$ (open symbols) and *Tcf7*$^{+/-}$ P14 Cond^{LacZ} cells (filled symbols) >day 60 after LCMV infection. (**D**) Abundance of the indicated *Tcf7*$^{-/-}$ (open symbols) and *Tcf7*$^{+/-}$ P14 memory subpopulation (filled symbols) >day 60 following LCMV infection. (*) and (**) depict significant differences ($p < 0.05$) and ($p < 0.01$), respectively, based on the Student *t* test.

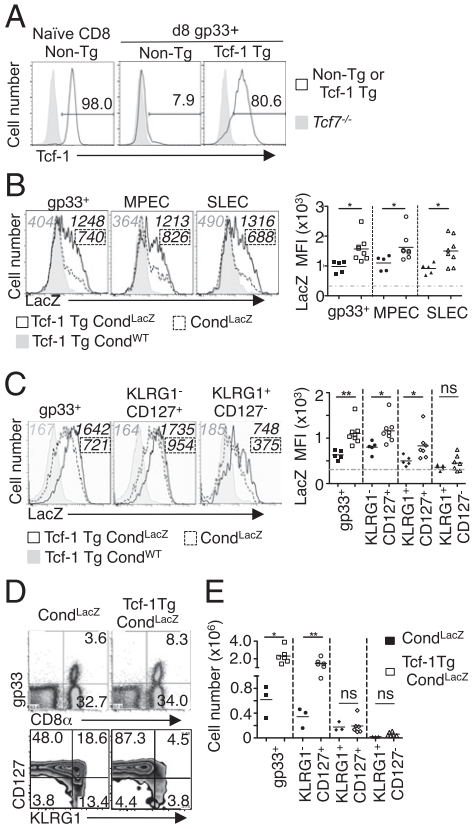

FIGURE 5. Downregulation of Tcf-1 limits conductin expression in effector CD8 T cells. (**A**) Intracellular Tcf-1 staining in naive CD8 T cells (*left*), in day 8 (d8) gp33-specific WT CD8 T cells (middle) and in d8 gp33-specific Tcf-1 Tg (p45 isoform) CD8 T cells (open histograms) relative to naive *Tcf7*$^{-/-}$ CD8 controls (gray fill). Roman numbers indicate the percent of cells in the respective gate. (**B**) Histogram overlays and the dot graph show Cond expression (LacZ activity) in total gp33 tetramer$^+$ CD8 T cells or MPEC or SLEC subpopulations from Tcf-1 Tg Cond^{LacZ} (black line) and Cond^{LacZ} mice (dashed line) relative to Cond^{WT} mice (gray fill) at d8 after LCMV infection. (**C**) Histogram overlays and dot graphs show Cond expression in total gp33 tetramer$^+$ memory cells and the indicated memory cell subsets at >day 40 after LCMV infection. (**D**) Density plots show the presence of gp33 tetramer$^+$ CD8 T cells in Tcf-1 Tg and non-Tg Cond^{LacZ} mice >day 40 after LCMV infection and their phenotype as defined by the differential expression of CD127 versus KLRG1. (**E**) Abundance of the indicated gp33 tetramer$^+$ memory (sub)-populations in the spleen of Tcf-1 Tg and non-Tg Cond^{LacZ} mice >day 40 after LCMV infection. Roman numbers indicate the percentage of cells in the respective gate or quadrant, and italic numbers depict the MFI of Cond expression of the corresponding population of cells. (*) and (**) depict significant differences ($p < 0.05$) and ($p < 0.01$), respectively, based on the Student *t* test.

the high Cond levels seen in WT CD127$^+$KLRG1$^-$ memory cells were significantly reduced in P14 cells lacking Tcf-1 (Fig.4B, 4C), and this memory cell subset was significantly reduced in number in the absence of Tcf-1 (Fig. 4D). These results show that Tcf-1 is required for efficient Wnt signal transduction in CD127$^+$KLRG1$^-$ memory cells. Inefficient Wnt signaling in the absence of Tcf-1 is associated with a reduced abundance of CD127$^+$KLRG1$^-$ memory cells, a decreased ability of memory cells to produce IL-2 (Supplemental Fig. 3B), and reduced re-expansion upon secondary challenge (Supplemental Fig. 3C), consistent with published data (2, 3).

Downregulation of Tcf-1 limits Wnt signal transduction in effector CD8 T cells

Wnt signal transduction was strongly reduced in most Ag-specific CD8 T cells during the primary immune response to LCMV infection (Fig. 1B). This coincided with reduced Tcf-1 expression in day 8 gp33$^+$ CD8 T cells (Fig. 5A) and in P14 cells from WT mice (Supplemental Fig. 4A). We thus tested whether the loss of Tcf-1 expression was responsible for the downregulation of Wnt signaling in effector cells using Tcf-1 (p45 isoform) Tg mice, in which Tcf-1 expression is controlled by heterologous regulatory elements (10). At day 8 following LCMV infection, Tcf-1 was expressed by a small subpopulation of gp33-specific CD8 T cells in non-Tg littermate mice, but was detected by essentially all gp33-specific CD8 T cells of Tcf-1 Tg mice (Fig. 5A**).** These data show that Tcf-1 loss during CD8 T cell effector differentiation is based on transcriptional control mechanisms. Cond expression was significantly increased among gp33-specific CD8 T cells of Tcf-1 Tg compared with littermate control mice, whereby elevated Cond levels were evident in both MPECs and SLECs (Fig. 5B). Moreover, whereas the magnitude of the gp33-specific CD8 T cell response was not altered, effector cell differentiation in Tcf-1 Tg mice was skewed toward MPECs, and this occurred at the expense

Downloaded from http://www.jimmunol.org/ at Bibliotheque Universitaire de Medecine on July 17, 2020

of SLECs (Supplemental Fig. 4B). Thus maintenance of Tcf-1 expression during the primary response enhanced Wnt signal transduction and limited SLEC differentiation, indicating that downregulation of Tcf-1 during the primary immune response limits Wnt signal transduction and facilitates terminal CD8 T cell differentiation.

Wnt signaling was also increased in Ag-specific KLRG1$^-$ CD127$^+$ memory cells of Tcf-1 Tg mice (Fig. 5C). This was associated with a 5-fold increase in the absolute number of CD127$^+$ KLRG1$^-$memory cells (Fig. 5D, 5E). Consistent with these findings, Tcf-1 Tg mice contained an enlarged pool of Ag-specific CD8 memory cells that produced IL-2 (Supplemental Fig. 4C). The transfer of equal numbers of gp33-specific CD8 memory cells into secondary recipients and challenge infection resulted in a recall expansion, which was comparable to that in controls (Supplemental Fig. 4D). Thus, on a per-cell-basis, supranormal Wnt signaling did not further enhance the re-expansion capacity. However, together with the increased number of memory cells, these data show that Tcf-1–mediated high Wnt signal transduction is associated with a significantly improved memory CD8 T cell compartment.

Discussion

In this article, we show that the canonical Wnt signaling pathway is constitutively active in essentially all naive CD8 T cells in vivo. Wnt signal transduction is strongly diminished in effector CD8 T cells around the peak of the expansion phase. These data indicate that downregulation of Wnt signaling is a late event during effector differentiation, likely unrelated to the initial clonal burst and the acquisition of effector function.

The transduction of canonical Wnt signals is initiated by the binding of extracellular Wnt proteins to Frizzled/LRP5/6 cell surface receptors. Signaling leads to the intracellular accumulation of nonphosphorylated (active) β-catenin (and likely γ-catenin), allowing β-catenin association with Tcf/Lef transcription factors, which serve as nuclear effectors of the pathways. Diminished Wnt signal transduction in effector cells was paralleled by multiple changes in responding CD8 T cells, including a reduced expression and activity of the Wnt coreceptor LRP6, a reduced expression of signaling-competent β-catenin, and a reduced expression of the nuclear effectors Tcf-1 and Lef-1. Enforced Tcf-1 expression enhanced Wnt signaling during the primary immune response, demonstrating that downregulation of Tcf-1 is shown to be responsible in part for the reduced Wnt signal transduction in effector cells.

The single-cell reporter analysis identified a subset of Ag-specific effector CD8 T cells, which maintained Cond expression during the primary response to infection. Of interest, even though reduced Wnt signal transduction coincided with progress toward terminal differentiation, low and high Wnt signaling coincided only in part with short-lived and MPECs, respectively. Adoptive transfer experiments showed that progeny of Cond$^-$ and Cond$^+$ effector cells had a comparable capacity to give rise to memory cells, but that Cond$^+$ cells showed significantly enhanced recall expansion capacity and conferred improved protection against viral infection, two hallmarks of central memory cells. Our data thus suggest that the maintenance of conductin expression, and thus Wnt signaling, among effector cells demarcates a precursor of central memory. Classical studies have shown that KLRG1$^+$ effector cells are relatively short lived, whereas KLRG1$^-$ effector cells showed improved persistence and generated both effector and central memory cells (18, 19). These data in conjunction with our findings raise the possibility that the combination of Cond and KLRG1 expression will allow a further discrimination of functionally relevant effector cell subpopulations. Although this remains to be tested, our data suggest that precursors of memory cells with distinct re-expansion potential can be identified during the primary CD8 T cell response based on differences in the transduction of Wnt signals rather than commonly used cell surface markers to discriminate effector T cell subpopulations.

During memory formation, Cond expression was observed in an increasing fraction of CD8 T cells, whereby Cond levels were significantly higher among KLRG1$^-$ than among effector-like KLRG1$^+$ or tissue-resident memory CD8 T cells. Even though the correlation between low and high Wnt signaling with effector and central memory phenotypes, respectively, was incomplete, memory CD8 T cells with elevated Wnt signal transduction displayed enhanced proliferative potential upon rechallenge. High Cond expression in KLRG1$^-$ memory CD8 T cells depended on Tcf-1, and the absence of Tcf-1 significantly reduced the abundance of KLRG1$^-$ memory cells. Conversely, enforced Tcf-1 expression enhanced Cond expression in memory cells and significantly expanded the pool of functional memory cells. Thus Tcf-1–dependent high levels of Wnt signal transduction were associated with the generation of KLRG1$^-$ memory cells with efficient recall expansion capacity.

Although naive and central memory cells have important qualitative differences, they share the ability to clonally expand. This property is lost in most effector cells and limited in effector memory and tissue-resident memory cells. Our data suggest that the maintenance of efficient Wnt signal transduction during the primary immune response preserves the capacity of the CD8 T cells to expand upon secondary stimulation. It may thus be possible to improve the formation of functional CD8 T cell memory during vaccination if Wnt signaling is maintained.

Acknowledgments

We thank C. Soneson (Swiss Institute for Bioinformatics Lausanne, Switzerland) for bioinformatic support; S. Luther (Department of Biochemistry, University of Lausanne) for discussion; the Flow Cytometry Facility and the Genomic Technologies Facility for expert assistance with flow cytometry and microarray experiments, respectively; P. Guillaume (TC Metrix) for tetramers; C. Mueller (University of Bern Bern, Switzerland) for LCMV strain WE; H. Clevers (University of Utrecht Utrecht, the Netherlands) for *Tcf7*$^{-/-}$ mice; H.P. Pircher (University of Freiburg Freiburg, Germany) for P14 mice; and N. Gardiol, A. Wicky, and members of the laboratory for help and discussion.

Disclosures

The authors have no financial conflicts of interest.

References

1. Kaech, S. M., and W. Cui. 2012. Transcriptional control of effector and memory CD8+ T cell differentiation. *Nat. Rev. Immunol.* 12: 749–761.
2. Jeannet, G., C. Boudousquié, N. Gardiol, J. Kang, J. Huelsken, and W. Held. 2010. Essential role of the Wnt pathway effector Tcf-1 for the establishment of functional CD8 T cell memory. *Proc. Natl. Acad. Sci. USA* 107: 9777–9782.
3. Zhou, X., S. Yu, D. M. Zhao, J. T. Harty, V. P. Badovinac, and H. H. Xue. 2010. Differentiation and persistence of memory CD8(+) T cells depend on T cell factor 1. *Immunity* 33: 229–240.
4. Zhou, X., and H. H. Xue. 2012. Cutting edge: generation of memory precursors and functional memory CD8+ T cells depends on T cell factor-1 and lymphoid enhancer-binding factor-1. *J. Immunol.* 189: 2722–2726.
5. Clevers, H., and R. Nusse. 2012. Wnt/β-catenin signaling and disease. *Cell* 149: 1192–1205.
6. Prlic, M., and M. J. Bevan. 2011. Cutting edge: β-catenin is dispensable for T cell effector differentiation, memory formation, and recall responses. *J. Immunol.* 187: 1542–1546.
7. Driessens, G., Y. Zheng, and T. F. Gajewski. 2010. Beta-catenin does not regulate memory T cell phenotype. *Nat. Med.* 16: 513–514, author reply 514–515.
8. Gattinoni, L., X. S. Zhong, D. C. Palmer, Y. Ji, C. S. Hinrichs, Z. Yu, C. Wrzesinski, A. Boni, L. Cassard, L. M. Garvin, et al. 2009. Wnt signaling arrests effector T cell differentiation and generates CD8+ memory stem cells. *Nat. Med.* 15: 808–813.

Downloaded from http://www.jimmunol.org/ at Bibliotheque Universitaire de Medecine on July 17, 2020

9. Verbeek, S., D. Izon, F. Hofhuis, E. Robanus-Maandag, H. te Riele, M. van de Wetering, M. Oosterwegel, A. Wilson, H. R. MacDonald, and H. Clevers. 1995. An HMG-box-containing T-cell factor required for thymocyte differentiation. *Nature* 374: 70–74.
10. Ioannidis, V., F. Beermann, H. Clevers, and W. Held. 2001. The β-catenin—TCF-1 pathway ensures CD4(+)CD8(+) thymocyte survival. *Nat. Immunol.* 2: 691–697.
11. Pircher, H., K. Bürki, R. Lang, H. Hengartner, and R. M. Zinkernagel. 1989. Tolerance induction in double specific T-cell receptor transgenic mice varies with antigen. *Nature* 342: 559–561.
12. Hogquist, K. A., S. C. Jameson, W. R. Heath, J. L. Howard, M. J. Bevan, and F. R. Carbone. 1994. T cell receptor antagonist peptides induce positive selection. *Cell* 76: 17–27.
13. Lustig, B., B. Jerchow, M. Sachs, S. Weiler, T. Pietsch, U. Karsten, M. van de Wetering, H. Clevers, P. M. Schlag, W. Birchmeier, and J. Behrens. 2002. Negative feedback loop of Wnt signaling through upregulation of conductin/axin2 in colorectal and liver tumors. *Mol. Cell. Biol.* 22: 1184–1193.
14. Battegay, M., S. Cooper, A. Althage, J. Bänziger, H. Hengartner, and R. M. Zinkernagel. 1991. Quantification of lymphocytic choriomeningitis virus with an immunological focus assay in 24- or 96-well plates. *J. Virol. Methods* 33: 191–198.
15. Subramanian, A., P. Tamayo, V. K. Mootha, S. Mukherjee, B. L. Ebert, M. A. Gillette, A. Paulovich, S. L. Pomeroy, T. R. Golub, E. S. Lander, and J. P. Mesirov. 2005. Gene set enrichment analysis: a knowledge-based approach for interpreting genome-wide expression profiles. *Proc. Natl. Acad. Sci. USA* 102: 15545–15550.
16. Jeannet, G., M. Scheller, L. Scarpellino, S. Duboux, N. Gardiol, J. Back, F. Kuttler, I. Malanchi, W. Birchmeier, A. Leutz, et al. 2008. Long-term, multilineage hematopoiesis occurs in the combined absence of beta-catenin and gamma-catenin. *Blood* 111: 142–149.
17. Jung, Y. W., R. L. Rutishauser, N. S. Joshi, A. M. Haberman, and S. M. Kaech. 2010. Differential localization of effector and memory CD8 T cell subsets in lymphoid organs during acute viral infection. *J. Immunol.* 185: 5315–5325.
18. Joshi, N. S., W. Cui, A. Chandele, H. K. Lee, D. R. Urso, J. Hagman, L. Gapin, and S. M. Kaech. 2007. Inflammation directs memory precursor and short-lived effector CD8(+) T cell fates via the graded expression of T-bet transcription factor. *Immunity* 27: 281–295.
19. Sarkar, S., V. Kalia, W. N. Haining, B. T. Konieczny, S. Subramaniam, and R. Ahmed. 2008. Functional and genomic profiling of effector CD8 T cell subsets with distinct memory fates. *J. Exp. Med.* 205: 625–640.
20. Kaech, S. M., S. Hemby, E. Kersh, and R. Ahmed. 2002. Molecular and functional profiling of memory CD8 T cell differentiation. *Cell* 111: 837–851.
21. Latner, D. R., S. M. Kaech, and R. Ahmed. 2004. Enhanced expression of cell cycle regulatory genes in virus-specific memory CD8+ T cells. *J. Virol.* 78: 10953–10959.

Downloaded from http://www.jimmunol.org/ at Bibliotheque Universitaire de Medecine on July 17, 2020